Interactions between octet baryons in the SU_6 quark model

Y. Fujiwara,[1] M. Kohno,[2] C. Nakamoto,[3] and Y. Suzuki[4]
[1]*Department of Physics, Kyoto University, Kyoto 606-8502, Japan*
[2]*Physics Division, Kyushu Dental College, Kitakyushu 803-8580, Japan*
[3]*Suzuka National College of Technology, Suzuka 510-0294, Japan*
[4]*Department of Physics, Niigata University, Niigata 950-2181, Japan*

(Received 22 June 2001; published 27 September 2001)

Baryon-baryon interactions for the complete baryon octet (B_8) are investigated in a unified framework of the resonating-group method, in which the spin-flavor SU_6 quark-model wave functions are employed. Model parameters are determined to reproduce properties of the nucleon-nucleon system and the low-energy cross section data for the hyperon-nucleon interaction. We then proceed to explore B_8B_8 interactions in the strangeness $S=-2$, -3, and -4 sectors. The S-wave phase-shift behavior and total cross sections are systematically understood by (1) the spin-flavor SU_6 symmetry, (2) the special role of the pion exchange, and (3) the flavor symmetry breaking.

DOI: 10.1103/PhysRevC.64.054001 PACS number(s): 13.75.Cs, 12.39.Jh, 13.75.Ev, 24.85.+p

I. INTRODUCTION

In the quark model, the baryon-baryon interactions for the complete octet baryons ($B_8 = N$, Λ, Σ, and Ξ) are treated entirely equivalently with the well-known nucleon-nucleon (NN) interaction. Once the quark-model Hamiltonian is assumed in the framework of the resonating-group method (RGM), explicit evaluation of the spin-flavor factors leads to the stringent flavor dependence appearing in various interaction pieces. We can thus minimize the ambiguity of the model parameters by utilizing the rich knowledge of the NN interaction.

In this study we first upgrade our previous model [1] for the NN and hyperon-nucleon (YN) interactions by incorporating more complete effective meson-exchange potentials (EMEP's) such as the vector mesons and some extra interaction pieces. This model is named fss2 [2] after the pioneering model FSS. Fixing the model parameters in the strangeness $S=0$ and -1 sectors, we proceed to explore the B_8B_8 interactions in $S=-2$, -3, and -4 sectors. These include the $\Lambda\Lambda$ and ΞN interactions, which have recently been attracting much interest in the rapidly developing fields of hypernuclear physics and strangeness nuclear matter.

In the next section, we recapitulate the formulation of the $(3q)$-$(3q)$ Lippmann-Schwinger RGM [3]. In Sec. III, we summarize the essential features of the NN and YN interactions, in order to furnish the basic components to understand the phase-shift behavior of the B_8B_8 interactions in a unified way. The model predictions of the B_8B_8 interactions in the $S=-2$, -3, and -4 sectors are given in Sec. IV, with respect to the S-wave phase shifts and the total cross sections. The final section is devoted to a summary.

II. FORMULATION

The quark-model Hamiltonian H consists of the phenomenological confinement potential $U_{ij}^{\rm Cf}$, the colored version of the full Fermi-Breit (FB) interaction $U_{ij}^{\rm FB}$ with explicit quark-mass dependence, and the EMEP $U_{ij}^{\Omega\beta}$ generated from the scalar ($\Omega = {\rm S}$), pseudoscalar (PS), and vector (V) meson-exchange potentials acting between quarks:

$$H=\sum_{i=1}^{6}\left(m_i c^2+\frac{\boldsymbol{p}_i^2}{2m_i}-T_G\right)+\sum_{i<j}^{6}\left(U_{ij}^{\rm Cf}+U_{ij}^{\rm FB}+\sum_{\beta}U_{ij}^{{\rm S}\beta}+\sum_{\beta}U_{ij}^{{\rm PS}\beta}+\sum_{\beta}U_{ij}^{{\rm V}\beta}\right). \tag{2.1}$$

It is important to include the momentum-dependent Bryan-Scott term [4] in the S- and V-meson contributions, in order to remedy the shortcoming of our previous model FSS; namely, the single-particle (s.p.) potential in nuclear matter is too attractive in the high-momentum region $k \gtrsim 6\ \mathrm{fm}^{-1}$. Another important feature of the present model is the introduction of vector mesons for improving the fit to the NN phase-shift parameters. Since the dominant effect of the ω-meson repulsion and the LS components of ρ, ω, and K^* mesons are already accounted for by the FB interaction, only the quadratic LS component of the octet mesons is expected to play an important role in partially canceling the strong one-pion tensor force. Further details of the model fss2 are given in [2]. The model parameters are fixed to reproduce the most recent results of the phase-shift analysis SP99 [5] for np scattering with partial waves $J \leqslant 2$ and incident energies $T_{\rm lab} \leqslant 350$ MeV, under the constraint of the deuteron binding energy and the $^1S_0$ NN scattering length, as well as the low-energy YN total cross section data. Owing to the introduction of the vector mesons, the model fss2 in the NN sector has attained an accuracy almost comparable to that of one-boson-exchange potential (OBEP) models. For example, the χ^2 values defined by $\chi^2 = \Sigma_{i=1}^{N}(\delta_i^{cal}-\delta_i^{expt})^2/N$ for the $J \leqslant 2$ phase-shift parameters in the energy range $T_{\rm lab} = 25$–300 MeV are $\sqrt{\chi^2} = 0.59°$, $1.10°$, $1.40°$, and $1.32°$ for fss2, OBEP, Paris, and Bonn, respectively. The existing data for the YN scattering are well reproduced and the essential feature of the ΛN-ΣN coupling is almost unchanged from our previous models.

TABLE I. The relationship between the isospin basis and the flavor-SU_3 basis for the B_8B_8 systems. The flavor-SU_3 symmetry is given by the Elliott notation $(\lambda\mu)$. $\mathcal{P}$ denotes the flavor-exchange symmetry and I the isospin.

S	$B_8B_8(I)$	$\mathcal{P}=+1$ (symmetric) ^1E or ^3O	$\mathcal{P}=-1$ (antisymmetric) ^3E or ^1O
0	$NN(I=0)$	–	(03)
	$NN(I=1)$	(22)	–
-1	ΛN	$\frac{1}{\sqrt{10}}[(11)_s+3(22)]$	$\frac{1}{\sqrt{2}}[-(11)_a+(03)]$
	$\Sigma N(I=1/2)$	$\frac{1}{\sqrt{10}}[3(11)_s-(22)]$	$\frac{1}{\sqrt{2}}[(11)_a+(03)]$
	$\Sigma N(I=3/2)$	(22)	(30)
-2	$\Lambda\Lambda$	$\frac{1}{\sqrt{5}}(11)_s+\frac{9}{2\sqrt{30}}(22)+\frac{1}{2\sqrt{2}}(00)$	–
	$\Xi N(I=0)$	$\frac{1}{\sqrt{5}}(11)_s-\sqrt{\frac{3}{10}}(22)+\frac{1}{\sqrt{2}}(00)$	$(11)_a$
	$\Xi N(I=1)$	$\sqrt{\frac{3}{5}}(11)_s+\sqrt{\frac{2}{5}}(22)$	$\frac{1}{\sqrt{3}}[-(11)_a+(30)+(03)]$
	$\Sigma\Lambda$	$-\sqrt{\frac{2}{5}}(11)_s+\sqrt{\frac{3}{5}}(22)$	$\frac{1}{\sqrt{2}}[(30)-(03)]$
	$\Sigma\Sigma$ $(I=0)$	$\sqrt{\frac{3}{5}}(11)_s-\frac{1}{2\sqrt{10}}(22)-\sqrt{\frac{3}{8}}(00)$	–
	$\Sigma\Sigma$ $(I=1)$	–	$\frac{1}{\sqrt{6}}[2(11)_a+(30)+(03)]$
	$\Sigma\Sigma$ $(I=2)$	(22)	–
-3	$\Xi\Lambda$	$\frac{1}{\sqrt{10}}[(11)_s+3(22)]$	$\frac{1}{\sqrt{2}}[-(11)_a+(30)]$
	$\Xi\Sigma$ $(I=1/2)$	$\frac{1}{\sqrt{10}}[3(11)_s-(22)]$	$\frac{1}{\sqrt{2}}[(11)_a+(30)]$
	$\Xi\Sigma$ $(I=3/2)$	(22)	(03)
-4	$\Xi\Xi$ $(I=0)$	–	(30)
	$\Xi\Xi$ $(I=1)$	(22)	–

The two-baryon systems composed of the complete baryon octet are classified as

$$1/2(11)\times 1/2(11)=\{0,\ 1\}\{(22)+(30)+(03)+(11)_s +(11)_a+(00)\}, \tag{2.2}$$

where $S(\lambda\mu)$ stands for the spin value S and the flavor SU_3 representation label $(\lambda\mu)$. If the space-spin states are classified by the flavor-exchange symmetry $\mathcal{P}$, the correspondence between the SU_3 basis and the isospin basis becomes very transparent, as in Table I. This correspondence is essential in the following discussion. The key point is that the quark-model Hamiltonian, Eq. (2.1), is approximately SU_3 scalar. If we ignore the EMEP terms $U^{\mathrm{S,PS,V}\beta}_{ij}$, this is fairly apparent since the flavor dependence appears only through the moderate mass difference of the up-down and strange quarks. In the FB interaction U^{FB}_{ij}, this is a direct consequence of the fact that the gluons do not have the flavor degree of freedom. In the EMEP terms, the SU_3 scalar property of the interaction is not apparent since the mesons have the flavor degree of freedom. Nevertheless, one can easily show that the interaction Hamiltonian is actually SU_3 scalar if the masses of the octet mesons are all equal within each of the S, PS, and V mesons. A nice feature of the quark model is that the approximate SU_3-scalar property of the total Hamiltonian is automatically incorporated in the model. On the other hand, in the OBEP a similar situation is only realized by assuming the SU_3 relations for the many baryon-meson coupling constants. If the Hamiltonian is exactly SU_3 scalar, the SU_3 states with a common $(\lambda\mu)$ in Table I should have the same baryon-baryon interaction. For example, the same (22) symmetry appears in several $^1S_0$ states, i.e., $NN(I=1)$, $\Sigma N(I=3/2)$, $\Sigma\Sigma(I=2)$, $\Xi\Sigma(I=3/2)$, and $\Xi\Xi(I=1)$. The $^1S_0$

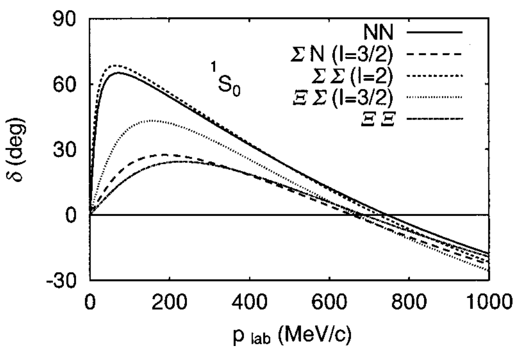

FIG. 1. $^1S_0$ phase shifts for the B_8B_8 interactions with the pure (22) state.

phase shifts of these channels have very similar behavior, as is shown in Fig. 1. In reality, the SU_3 symmetry is broken, but in a very specific way. The mechanism of the flavor symmetry breaking (FSB) depends on the details of the model. In the present framework, the following three factors cause FSB.

(1) The strange to up-down quark mass ratio $\lambda = m_s/m_{ud} = 1.551$ (for fss2)>1 in the kinetic-energy term and $U_{ij}^{\rm FB}$.

(2) The singlet-octet meson mixing in $U_{ij}^{\rm S,PS,V\beta}$.

(3) The meson and baryon mass splitting in $U_{ij}^{\rm S,PS,V\beta}$ and the kinetic-energy term, and the resultant difference of the threshold energies.

III. CHARACTERISTICS OF THE *NN* AND *YN* INTERACTIONS AND THE BASIC VIEWPOINT

The approximate SU_3-scalar property of the Hamiltonian implies that accurate knowledge of the *NN* and *YN* interactions is crucial to understand the B_8B_8 interactions in the $S = -2$, -3, and -4 sectors. The following four points concerning the qualitative behavior of the *NN* and *YN* interactions are essential [1,2]. First, in the *NN* system the $^1S_0$ state with isospin $I=1$ consists of the pure (22) state, and the phase shift shows a clear resonance behavior reaching more than 60° (see Fig. 1). On the other hand, the $^3S_1$ state with $I=1$ is composed of the pure (03) state, and the deuteron is bound in this channel owing to the strong one-pion tensor force. If we switch off this strong tensor force, the ^3S phase shift rises to 20°–30° at most, indicating that the central attraction of the (03) state is not as strong as that of the (22) state (see crosses in Fig. 2). Detailed analysis of the *YN* interaction has clarified that the $(11)_s$ state for the $^1S_0$ state and the (30) state for the $^3S_1$ state are both strongly repulsive, reflecting that the most compact $(0s)^6$ configuration is completely Pauli forbidden for the $(11)_s$ state and almost forbidden for the (30) state [6]. The repulsive behavior of the $\Sigma N(I=3/2)^3S_1$ state with the pure (30) symmetry should be observed as a strong isospin dependence of the Σ s.p. potential. On the other hand, the experimental evidence of the repulsion is not clear for the $\Sigma N(I=1/2)$ $^1S_0$ state, which contains 90% $(11)_s$ component. This is because the observables are usually composed of the contributions both from

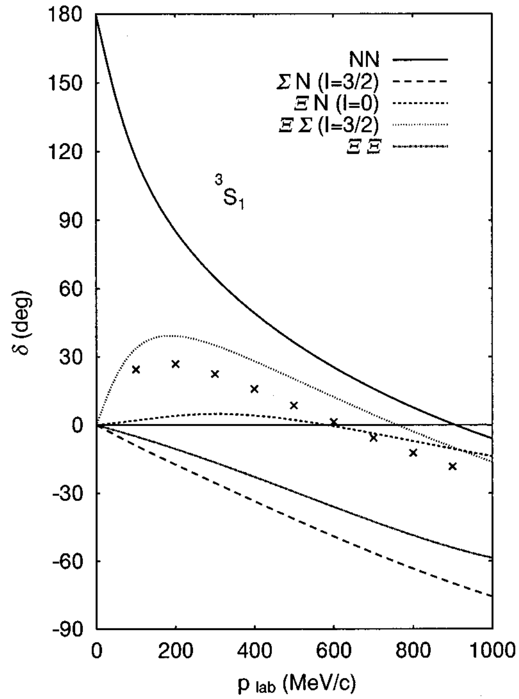

FIG. 2. $^3S_1$ phase shifts for the (03) $[NN, \Xi\Sigma(I=3/2)]$, $(11)_a$ $[\Xi N(I=0)]$, and (30) $[\Sigma N(I=3/2), \Xi\Xi]$ states. The ^3S phase shift predicted only by the *NN* central interaction is also shown by crosses.

the $^1S_0$ and $^3S_1$ states, and the $^3S_1$ state in this channel involves a rather cumbersome ΛN-$\Sigma N(I=1/2)$ channel coupling. Nevertheless, the repulsive character of the $(11)_s$ state is not inconsistent with the present experimental evidence, in the sense that FSS and fss2 reproduce the available low-energy cross section data of the Λp and $\Sigma^- p$ scatterings quite well. The strength of this repulsion depends on the detailed framework of the quark model. In the OBEP approach, even the qualitative features of these interactions are sometimes not reproduced. For example, in the $\Sigma N(I=3/2)$ $^3S_1$ state almost all the Nijmegen soft-core models [7,8] predict a broad resonance around the intermediate-energy region of $p_\Sigma \sim 400$–600 MeV, although the low-energy behavior of the phase shifts is surely repulsive.

The following two additional features of the present

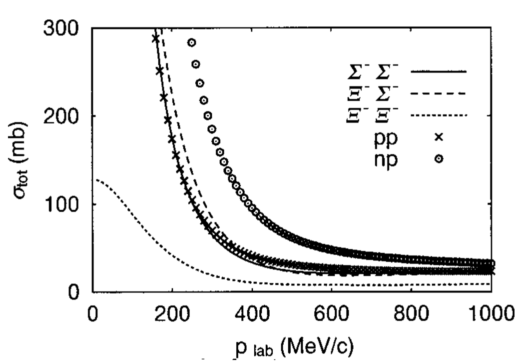

FIG. 3. Total elastic cross sections for the pure (22) state $(pp, \Sigma^-\Sigma^-, \Xi^-\Xi^-)$ and for the (22)+(03) states $(np, \Xi^-\Sigma^-)$.

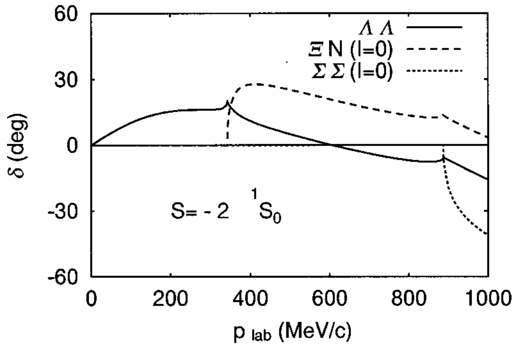

FIG. 4. $^1S_0$ phase shifts in the $\Lambda\Lambda$-ΞN-$\Sigma\Sigma$ coupled-channel system with $I=0$.

model should be kept in mind during the discussion of the B_8B_8 interactions in the $S=-2$, -3, and -4 sectors. First, the flavor-singlet (00) state which appears in the $S=-2$ sector for the first time is usually attractive in the quark model, owing to the $(\boldsymbol{\sigma}_1\cdot\boldsymbol{\sigma}_2)(\lambda_1^C\lambda_2^C)$-type color-magnetic interaction involved in $U_{ij}^{\rm FB}$. Whether the H-dibaryon state with the pure (00) is bound or not depends on how much the strangeness-exchange EMEP contribution cancels the strong channel coupling effect from the FB interaction $U_{ij}^{\rm FB}$ [9]. Next, the $(11)_a$ configuration which appears in the $S=-1$ sector partially appears in the $^3S_1$ state in $\Xi N(I=0)$ in the pure SU_3 form. The fss2 prediction for the phase shift of this interaction, depicted in Fig. 2, implies that this interaction is very weak, since the phase-shift rise is only 5°. Nevertheless, the phase-shift behavior of the $^3S_1$ states for the ΛN and $\Sigma N(I=1/2)$ channels in the $S=-1$ sector is very different [1,2]. This is apparently due to the strong effect of the one-pion tensor force, which is present in the ΣN channel, while absent in the ΛN channel. We can therefore conclude that a further important factor besides the FSB is the specific effect of the Goldstone-boson pions, which is very much channel dependent. As a consequence of the SU_3 relations, the role of the pion is generally reduced if the strangeness involved in the system increases.

IV. RESULTS IN $S=-2$, -3, AND -4 SECTORS

Table I shows a "reflection" symmetry with respect to the interchange between $S=0$ and $S=-4$ sectors and, also, between $S=-1$ and $S=-3$ sectors. Just like the particle-hole symmetry in the nuclear shell model, the SU_3 state on one side is obtained from the $(\lambda\mu)$ state on the other side by simply interchanging the λ and μ. Since the (22) [and also $(11)_s$] symmetry in the $^1S_0$ state returns to itself, the NN, ΛN, and ΣN interactions with N being replaced by Ξ should be very similar to the original ones. On the other hand, in the $^3S_1$ state the (03) symmetry changes into the (30) symmetry and the attractive interaction turns to the repulsive one. For example, the $\Xi\Xi(I=0)$ interaction with the pure (30) symmetry is repulsive. Figure 3 shows that the $\Xi\Xi$ total cross sections are about 1/4–1/5 of the NN cross sections. This result is different from the very large prediction of the Nijmegen soft-core potentials in [10], which have strong attractions in all the (22) channels except for the NN and Σ^+p ones. Among the strangeness B_8B_8 channels having the $^1S_0$ (22) configuration, the most attractive $^3S_1$ state is expected for the $\Xi\Sigma(I=3/2)$ interaction. Table I shows that this interaction has a very interesting feature: the two SU_3 symmetries (22) and (03) in the NN interaction appear in a common isospin state $I=3/2$. Unlike the (03) state in NN, the (03) state in $\Xi\Sigma(I=3/2)$ is only moderately attractive, since the $\Xi\Sigma$ system does not allow the strong one-pion exchange in the exchange Feynman diagram. Even in the direct Feynman diagram, the inclusion of the strangeness reduces the one-pion-exchange effect drastically through the SU_3 relations. The $\Xi^-\Sigma^-$ interaction thus gives the largest total cross sections in the strangeness sector, together with the $\Sigma^-\Sigma^-$ interaction, as seen in Fig. 3. The magnitudes of these total cross sections, however, are at most comparable with the pp total cross sections. The $\Xi\Lambda$-$\Xi\Sigma(I=1/2)$ coupled-channel problem, on the other hand, is less interesting, since the one-pion tensor force in the $^3S_1+{}^3D_1$ state becomes less effective due to the strong repulsion of the (30) component. This is in contrast with the strong ΛN-$\Sigma N(I=1/2)$ channel coupling, which leads to the well-known cusp structure in the ΛN total cross sections.

The baryon-baryon interactions in the $S=-2$ sector constitute the most difficult case to analyze, involving three different types of two-baryon configurations: $\Lambda\Lambda$-ΞN-$\Sigma\Sigma$ for $I=0$ and ΞN-$\Sigma\Lambda$-$\Sigma\Sigma$ for $I=1$. In this case, the isospin dependence of the interaction is very important, just as in the $\Sigma N(I)$ interactions with $I=1/2$ and 3/2. Figure 4 shows the $^1S_0$ phase-shift behavior of the full $\Lambda\Lambda$-ΞN-$\Sigma\Sigma$ coupled-channel system with $I=0$, in which the H-dibaryon bound state might exist. In the previous model FSS the $\Lambda\Lambda$ phase shift rises to 40° [11], while in the present fss2 it rises only to $\sim 20°$ at most. The situation is the same as in the $\Xi N(I$

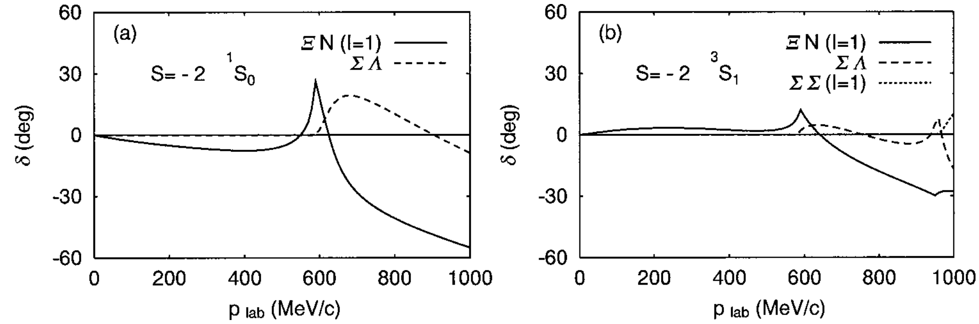

FIG. 5. (a) $^1S_0$ phase shifts in the ΞN-$\Sigma\Lambda$-$\Sigma\Sigma$ coupled-channel system with $I=1$. (b) The same as (a) but for the $^3S_1$ state.

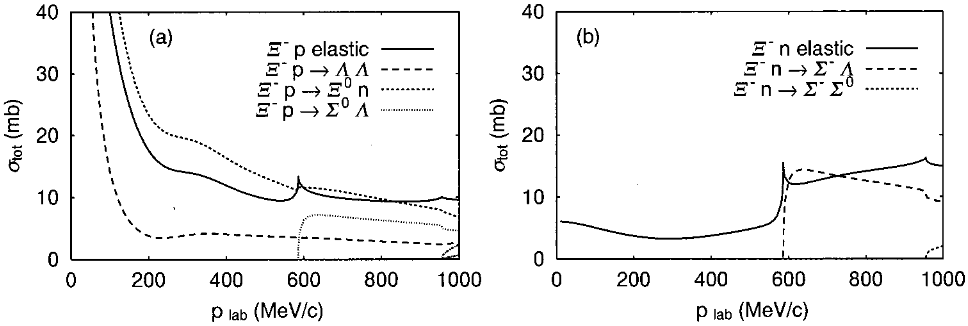

FIG. 6. (a) Total cross sections for $\Xi^- p$ scattering with $I=0$ and 1 contributions. (b) The same as (a) but for $\Xi^- n$ scattering only with the $I=1$ contribution.

$=0$) phase shift. It rises only to 30°–40° in fss2. Table I shows that the largest contribution of the (00) component is realized not in the $\Lambda\Lambda$ channel, but in the $\Xi N(I=0)$ channel. This implies that the attractive effect of the (00) configuration is smaller in fss2 than in FSS. Since FSS does not have the H-dibaryon bound state [11], fss2 does not have it either. As to the $\Lambda\Lambda$ interaction, it has been claimed that a phase-shift rise on the order of 40° is at least necessary to explain the known three events of the double Λ hypernuclei. However, the recently discovered "Demachi-Yanagi event" [12] for ${}^{10}_{\Lambda\Lambda}$Be ande "Nagara event" [13] for ${}^{6}_{\Lambda\Lambda}$He indicate that the $\Lambda\Lambda$ interaction is less attractive. A rough estimate of $\Delta B_{\Lambda\Lambda}$ for ${}^{6}_{\Lambda\Lambda}$He in terms of the G-matrix calculation using fss2 is about 1 MeV, which is consistent with this experimental observation.

In the isospin $I=1$ channel, the lowest incident baryon channel in the $S=-2$ sector is the ΞN channel. Figure 5 shows the phase-shift behavior of the ${}^1S_0$ and ${}^3S_1$ states, calculated for the full coupled-channel system ΞN-$\Sigma\Lambda$-$\Sigma\Sigma$ with $I=1$. In the $\Xi N(I=1)$ single-channel calculation, both of these phase shifts show monotonic repulsive behavior, originating from the main contributions of the $(11)_s$ and (30) components, respectively [9]. In the full coupled-channel calculation, however, the channel-coupling effect between $\Xi N(I=1)$ and $\Sigma\Lambda$ channels is enhanced by the cooperative role of the FB contribution $U_{ij}^{\rm FB}$ and EMEP contribution $U_{ij}^{\Omega\beta}$ in the strangeness-exchange process. As a result, the $\Xi N(I=1)$ phase shifts show very prominent cusp structure at the $\Sigma\Lambda$ threshold, as seen in Fig. 5. Below the $\Sigma\Lambda$ threshold, the phase-shift values are almost zero. Subsequently, the $\Xi^0 p$ (and $\Xi^- n$) total cross sections with the pure $I=1$ component are predicted to be very small below the $\Sigma\Lambda$ threshold around $p_\Xi \sim 600$ MeV/c. This behavior of the $\Xi^- n$ total cross sections, illustrated in Fig. 6(b), is essentially the same as the Nijmegen result in [10]. On the other hand, the $\Xi^- p$ total cross sections, shown in Fig. 6(a), exhibit a typical channel-coupling behavior similar to that of the $\Sigma^- p$ total cross sections. These features demonstrate that the $\Sigma\Lambda$ channel-coupling effect is very important for the correct description of scattering observables, resulting in the strong isospin dependence of the ΞN interaction.

V. SUMMARY

The conversion processes among octet baryons B_8 are most straightforwardly incorporated in the coupled-channel formalism. Since our quark model Hamiltonian is approximately SU_3 scalar, it is crucial to clarify the characteristics of the B_8B_8 interaction for each of the SU_3 states, rather than for each of the two-baryon systems. An interbaryon potential in a single-baryon channel is sometimes used for the study of hypernuclei and strangeness nuclear matter. However, such effective interactions are very much model dependent and linkage to the bare interactions like the ones discussed here is sometimes obscured by inherent ambiguities originating from the many-body calculations. The widespread argument that the hypernuclear structure reflects the hyperon-nucleon (YN) interaction rather faithfully since the YN interaction is weak should not be overemphasized.

In this study we have upgraded our previous quark model [1] for the nucleon-nucleon (NN) and YN interactions by incorporating more complete effective meson-exchange potentials such as the vector mesons and some extra interaction pieces. This model, fss2 [2], reproduces the existing data of the NN and YN interactions quite well. We have then proceeded to predict all the B_8B_8 interactions in the strangeness $S=-2$, -3, and -4 sectors, without adding any extra parameters. We have discussed some characteristic features of the B_8B_8 interactions, focusing on the qualitative aspect. Among these features are the following: (1) There is no bound state in the B_8B_8 systems, except for the deuteron. (2) The $\Xi\Xi$ total cross sections are far smaller than the NN cross sections. (3) The ΞN interaction has a strong isospin dependence similar to the ΣN system. (4) The $\Xi^-\Sigma^-[\Xi\Sigma(I=3/2)]$ interaction is moderately attractive. The S-wave phase-shift behavior yielding these qualitative features of the B_8B_8 interactions is systematically understood by (1) the spin-flavor SU_6 symmetry, (2) the special role of pion exchange, and (3) the flavor symmetry breaking. A more detailed analysis of the B_8B_8 interactions consistent with the available experimental data will be published in a forthcoming paper.

ACKNOWLEDGMENTS

This research was supported by Japan Grant-in-Aid for Scientific Research from the Ministry of Education, Science, Sports and Culture (12640265).

[1] Y. Fujiwara, C. Nakamoto, and Y. Suzuki, Phys. Rev. Lett. **76**, 2242 (1996); Phys. Rev. C **54**, 2180 (1996).
[2] Y. Fujiwara, T. Fujita, M. Kohno, C. Nakamoto, and Y. Suzuki, Few-Body Syst., Suppl. **12**, 311 (2000); Report No. KUNS-1703, nucl-th/0101014.
[3] Y. Fujiwara, M. Kohno, T. Fujita, C. Nakamoto, and Y. Suzuki, Prog. Theor. Phys. **103**, 755 (2000).
[4] R.A. Bryan and B.L. Scott, Phys. Rev. **164**, 1215 (1967).
[5] Scattering Analysis Interactive Dial-up (SAID), Virginia Polytechnic Institute, Blacksburg, Virginia; R. A. Arndt (private communication).
[6] C. Nakamoto, Y. Suzuki, and Y. Fujiwara, Prog. Theor. Phys. **94**, 65 (1995).
[7] P.M.M. Maessen, Th.A. Rijken, and J.J. de Swart, Phys. Rev. C **40**, 2226 (1989).
[8] Th.A. Rijken, V.G.J. Stoks, and Y. Yamamoto, Phys. Rev. C **59**, 21 (1999).
[9] C. Nakamoto, Y. Suzuki, and Y. Fujiwara, Prog. Theor. Phys. **97**, 761 (1997).
[10] V.G.J. Stoks and Th.A. Rijken, Phys. Rev. C **59**, 3009 (1999).
[11] C. Nakamoto, Y. Fujiwara, and Y. Suzuki, Nucl. Phys. **A670**, 315c (2000).
[12] A. Ichikawa, Ph.D. thesis, Kyoto University, 2000.
[13] H. Takahashi (private communication).